Bull. Hiroshima Inst. Tech. Research Vol. 60 (2026) 89-96

Article

Development of a simplified wavelength standard using stabilized 894 nm single-mode VCSEL with dichroic atomic vapor laser lock

Yuya BONKOHARA * and Leo MATSUOKA **

(Received October 31, 2025)

Abstract

We have developed a low-cost and simplified absolute wavelength standard for the cesium D_1 line (894 nm) using a single-mode vertical-cavity surface-emitting laser (VCSEL) stabilized by a dichroic atomic vapor laser lock (DAVLL). The DAVLL signal, obtained from the differential transmission of two orthogonal circular polarizations through cesium vapor in an external magnetic field, was optimized by adjusting the number and arrangement of ring-shaped permanent magnets. Using this optimized signal, a feedback control system was implemented to stabilize the VCSEL wavelength, resulting in a measured drift rate of 0.57 ± 0.01 kHz/s. These results suggest that using the stabilized VCSEL as a wavelength standard is effective for experiments that require determining the wavelength of another laser within a GHz-scale spectral region, with a precision better than 10 MHz for peak determination, despite the 50 MHz linewidth of the DAVLL signal, in situations where continuous scanning is not available.

Key Words: Laser, Spectroscopy, Wavelength stabilization, Zeeman-selective optical pumping

1 Introduction

Since its invention, the laser has advanced many areas of science and technology and has become an essential tool in modern society [1]. In particular, laser cooling and trapping of atoms have played a key role in the development of experimental quantum mechanics, achievements that were recognized with the Nobel Prizes in Physics in 1997 and 2001 [2, 3]. While sophisticated laser systems for controlling cold atoms in isolated environments have achieved remarkable progress, the use of lasers for studying and controlling more complex systems—such as plasmas or high-temperature atomic ensembles with thermal distribution—remains an important subject in applied spectroscopy. Recent progress in semiconductor lasers, especially their low cost and ease of operation, has further broadened the scope of applications in this field.

When performing spectroscopy or investigating wavelength-dependent phenomena with lasers, a reliable wavelength standard is required. Absolute wavelengths are usually calibrated using atomic transitions, while relative values and linearity are calibrated with interferometers. If measurements involve continuous wavelength scanning, calibration can be achieved easily by simultaneously recording several atomic transition signals or interferometer fringes. In contrast, when working at a fixed laser wavelength, a reference laser can serve as the wavelength standard by injecting both the reference and the experimental laser into the same scanning etalon. The wavelength of the experimental laser is then determined in real time from the difference in their peak positions. For this method to be effective, the reference laser itself must be stabilized to an

* Graduate School, Hiroshima Institute of Technology, Hiroshima, Hiroshima 731-5193, Japan
** Faculty of Engineering, Hiroshima Institute of Technology, Hiroshima, Hiroshima 731-5193, Japan

absolute standard such as an atomic transition.

To stabilize a laser's wavelength, an error signal that indicates the deviation from a reference is required. The simplest way to generate such a signal from atomic transitions is side fringe locking on an absorption line. However, this method is very sensitive to changes in vapor pressure caused by temperature fluctuations. More advanced techniques, such as modulation transfer spectroscopy (MTS) [4-6], are highly effective for stabilizing lasers with intrinsically narrow linewidths. At the same time, they require expensive components, including electro-optic modulators (EOMs) and lock-in amplifiers. In addition, the lock-in process involves integration time. These factors make MTS less suitable for stabilizing lasers that are inherently unstable.

Dichroic atomic vapor laser lock (DAVLL) [7-11] offers a cost-effective method for wavelength stabilization and is particularly suitable for suppressing wavelength drift in unstable lasers. In this technique, a magnetic field is applied along the laser propagation direction, introducing circular dichroism in the atomic medium. The differential signal between the two circular polarization components then serves as the error signal.

Unlike frequency modulation or lock-in amplification methods, DAVLL does not require modulation. It also allows flexible tuning of the lock point over a relatively broad frequency range, making it easy to use. Furthermore, the influence of vapor pressure fluctuations on signal amplitude is largely canceled in the differential measurement, which makes DAVLL more robust against temperature variations than side-fringe locking. The use of permanent magnets reduces flexibility in optimizing the magnetic field distribution, but it also eliminates heating effects that occur with current-driven coils.

Several enhanced versions of DAVLL have been reported, including tilted DAVLL (t-DAVLL) [12, 13], small-sized DAVLL [14], and sub-Doppler DAVLL [13, 15]. Nevertheless, even standard DAVLL is sufficient for developing a simplified wavelength-standard laser.

Vertical-cavity surface-emitting lasers (VCSELs) were first developed in 1997 [16]. They are a type of semiconductor laser that emits light perpendicular to the substrate. Owing to their manufacturing process, which is suitable for mass production, VCSELs are more cost-effective than conventional edge-emitting lasers. In recent years, single-mode VCSELs, capable of emitting at a single wavelength, have become widely available, although the choice of available wavelengths remains limited.

VCSELs are highly resistant to temperature variations and allow continuous wavelength tuning over a broad range without mode hopping by adjusting the injection current. However, they have relatively low output power, and their sensitivity to current noise can broaden the emission linewidth, which is a disadvantage. Because of these characteristics, VCSELs are well-suited for spectroscopy of atomic or plasma systems in which Doppler broadening is dominant. Their low output power also makes them suitable for use as simplified wavelength standards in applications where high power is not required.

In this study, we developed a cost-effective and straightforward absolute wavelength reference using a VCSEL-DAVLL system for the cesium D_1 line at 894 nm. Our research on light-induced drift (LID) [17] in cesium atoms requires investigating wavelength-dependent effects over a ~2 GHz range near the absorption line, without continuous laser wavelength scanning. The system developed here functions as a subsystem for LID experiments, providing a stable wavelength reference that enables efficient data acquisition while keeping both complexity and cost low.

2 Experimental methods

2.1 Principle of DAVLL

The principle of Dichroic Atomic Vapor Laser Lock (DAVLL) has been well described in previous studies [7, 8], so only a brief overview is given here. Figure 1 illustrates the generation of an ideal DAVLL signal using absorption spectroscopy. When a magnetic field is applied along the propagation direction of a linearly polarized laser beam, the atomic medium exhibits dichroism with respect to the two circular polarization components that make up the linear polarization. One component's absorption shifts to higher frequencies,

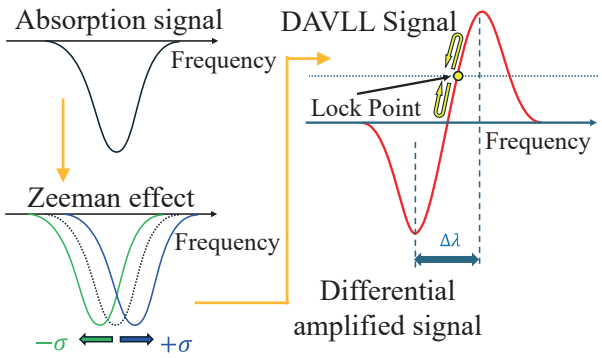

Fig. 1. Conceptual illustration of ideal DAVLL signal formation using laser absorption spectroscopy. $\Delta\lambda$ indicates the capture range of the frequency lock.

while the other shifts to lower frequencies.

A quarter-wave plate converts the intensity ratio of the two circular polarization components into a ratio of horizontal and vertical polarization components, which are then separated using a polarization beam splitter. The differential absorption spectra of these separated components are used to generate an error signal, hereafter referred to as the DAVLL signal. This signal serves as feedback for wavelength stabilization. The gradient of the DAVLL signal determines the sensitivity of the frequency lock, i.e., how quickly the feedback loop can respond, while the amplitude determines the capture range and the stability of the lock.

For transitions with hyperfine structures, such as the D_1 and D_2 lines of cesium-133, the absorption spectrum's response to the magnetic field becomes more complex. To obtain a clean DAVLL signal, it is necessary to optimize the magnetic field strength. In this study, the magnetic field was generated using ring-shaped permanent magnets, and the optimal configuration was determined by adjusting the number and arrangement of the magnets.

2.2 Experimental Apparatus

Figure 2 shows the setup for the VCSEL-DAVLL experiment. The vertical-cavity surface-emitting laser (VCSEL, L895VH1, Thorlabs) was mounted on a laser holder (TCLDM9, Thorlabs) and driven by a current controller (LDC200C, Thorlabs) and a temperature controller (TED200C, Thorlabs). The injection current was modulated using a function generator (WF1974, NF Corporation). To minimize back-reflections and

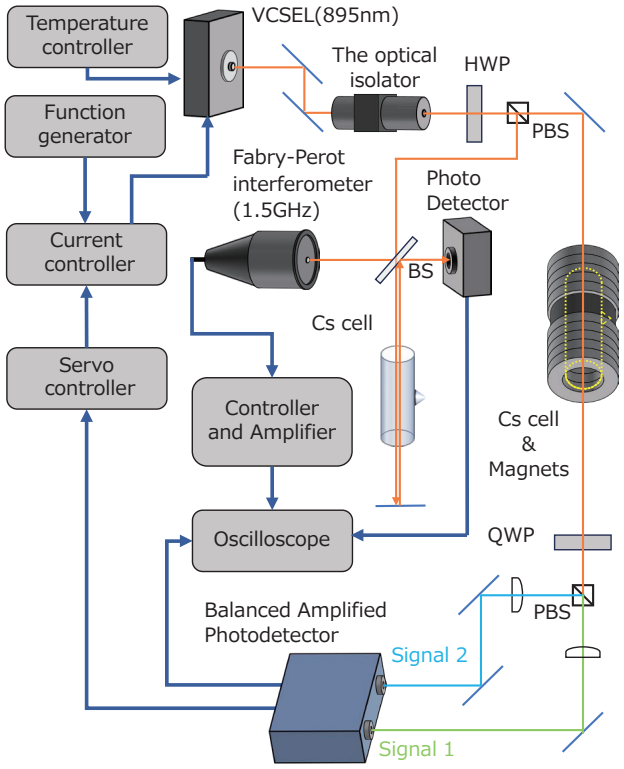

Fig. 2. Schematic of the DAVLL system. HWP, QWP, and PBS denote the half-wave plate, quarter-wave plate, and polarizing beam splitter, respectively. The combination of the HWP and PBS splits the laser beam, enabling simultaneous generation of the DAVLL signal and saturated absorption spectroscopy. The QWP and PBS are used to separate the circular polarizations of Signal 1 and Signal 2. The DAVLL signal is generated from these two signals, and feedback is provided to the laser's current controller through a servo controller to stabilize the wavelength.

ensure stable operation, an optical isolator (I-80-U-4-L, ISOWAVE) was placed after the VCSEL. The laser output was split for power adjustment using a $\lambda/2$ plate and a polarizing beam splitter (PBS), with part of the light directed to the monitoring line.

The linearly polarized laser was passed through a cesium vapor cell (100 mm long, 30 mm diameter; Horizon) placed at the center of a ring-shaped permanent magnet (8 mm thick). The average magnetic field strength at the cell position was measured to be 356.5 G. After passing through the gas cell, the laser light was processed by a $\lambda/4$ plate and PBS to convert the circular polarization into linear polarization components (horizontal and vertical). These components were then measured with a differential amplifier photodetector (Nirvana Detector Model 2007, New Focus) to generate the DAVLL signal. This signal was fed back into the laser current controller through a servo controller (LB1005, New

Focus), stabilizing the laser wavelength.

To focus the laser onto the photodetector, a 100 mm focal length plano-convex lens was used. For relative frequency calibration, the DAVLL signal was acquired alongside the signal from a Fabry–Perot interferometer (SA30-95, THORLABS, FSR: 1.5 GHz) using an oscilloscope (DHO924, RIGOL). The laser beam, split by a beam splitter, was passed through the cesium gas cell, and the reflected light was used to scan the saturated absorption spectrum with the photodetector. The output laser power was measured with a power meter (PM100D, Thorlabs), and the approximate VCSEL wavelength was measured with a wavelength meter (SHR, Solar Laser Systems).

3 Results

First, we describe the output characteristics of the VCSEL used in this experiment. Inexpensive VCSELs often exhibit variations in their output wavelength. Figure 3 (a) shows the relationship between the driving current (horizontal axis) and the wavelength measured with a wavelength meter (vertical axis). The temperature controller was set to 44.00 °C, and cesium absorption was observed around 2.67 mA. The wavelength increased linearly with current, with a slope of 0.335 nm/mA. Although not plotted in the figure, the output power also exhibited a linear dependence on current, ranging from 0.003 mW at the lowest current to 0.2 mW at the highest, corresponding to a slope of 0.089 mW/mA. These results indicate that a single-mode VCSEL can achieve continuous wavelength scanning of approximately 0.6 nm under a fixed-temperature setting.

Figure 3 (b) shows the dependence of the VCSEL wavelength on temperature at a fixed driving current of 2.610 mA. The horizontal axis represents the laser temperature, and the vertical axis represents the wavelength measured with a wavelength meter. Cesium absorption was observed when the VCSEL temperature was set to 44℃. The wavelength increased linearly with temperature, with a slope of 0.070 nm/°C. These results demonstrate that a single-mode VCSEL allows for wavelength tuning of about 3.5 nm by adjusting the operating temperature within a range

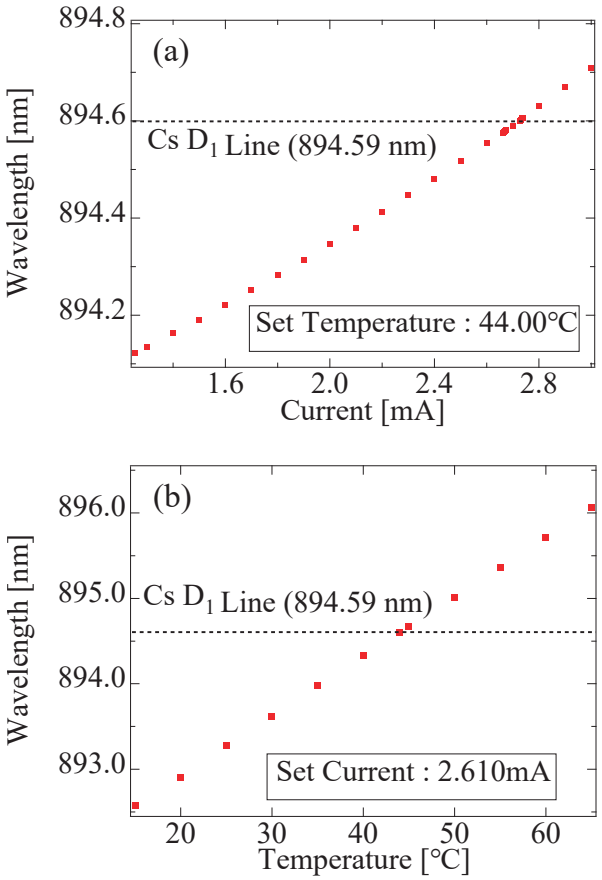

Fig. 3. Wavelength variations of the VCSEL with changes in (a) driving current at a fixed temperature of 44.00 ° C and (b) laser temperature at a fixed driving current of 2.610 mA, where cesium (Cs) absorption is observed.

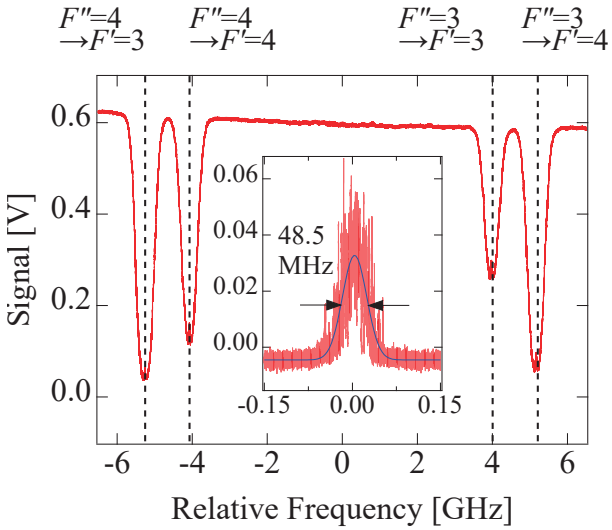

Fig. 4. Absorption spectrum (measured by saturated absorption spectroscopy) and Fabry–Perot interferometer measurement using the VCSEL. The red line shows the absorption spectrum obtained with the VCSEL, where the four peaks correspond to the hyperfine structure of the cesium D_1 line. The inset presents the laser linewidth of the VCSEL (red line) together with a fitted Gaussian distribution (blue line).

close to room temperature. The actual tunable range varies between individual VCSEL units, even of the same model, with an uncertainty of approximately 2 nm in the central wavelength.

Figure 4 shows the absorption spectrum obtained with the VCSEL. The horizontal axis represents the relative frequency measured with a Fabry–Perot interferometer, and the vertical axis represents the signal intensity detected by an amplified photodetector. The VCSEL wavelength was scanned by varying the driving current.

In the cesium D_1 line, four Doppler-broadened peaks were observed, corresponding to the hyperfine transitions $F''=4 \rightarrow F'=3$, $F''=4 \rightarrow F'=4$, $F''=3 \rightarrow F'=3$, and $F''=3 \rightarrow F'=4$. At the center of each peak, absorption decreased due to saturation effects. These results demonstrate that VCSEL wavelength scanning by current modulation provides sufficient resolution to resolve features as narrow as the Doppler linewidth (~500 MHz). Furthermore, the ability to scan across the entire hyperfine structure of the cesium D_1 line (~10 GHz) in a single sweep without mode hopping highlights the advantages and ease of use of VCSELs, whereas external-cavity semiconductor lasers typically allow a tuning range of only about 3 GHz.

The inset in the center of Figure 4 shows the VCSEL spectrum measured with a Fabry–Perot interferometer. Owing to significant current noise, the VCSEL exhibited a full width at half maximum (FWHM) linewidth of 48.5 MHz—more than ten times broader than the typical linewidth of an external-cavity laser (~1 MHz). This broad linewidth makes VCSELs less suitable for resolving fine structures in saturated absorption spectra. The spectrum shown in the inset is from a single-shot measurement; averaging would reduce the apparent noise. In the following, we describe wavelength stabilization of the VCSEL using feedback control. Although narrowing the linewidth remains a challenge, the primary objective here is to suppress wavelength drift rather than to reduce the linewidth.

Figure 5 presents a set of graphs showing the DAVLL signal, Signal 1, and Signal 2, with relative frequency on the horizontal axis and signal voltage on the vertical axis, organized according to the number and arrangement of magnets. The magnet

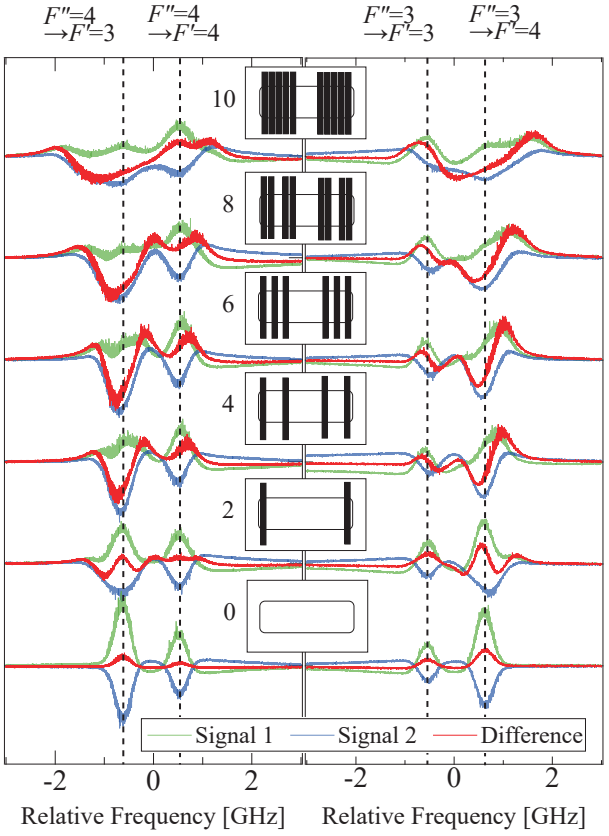

Fig. 5. Changes in the DAVLL signal corresponding to the number and arrangement of magnets. The green and blue lines represent the absorption of the two circularly polarized light components, while the red line shows the differential signal.

configurations are shown in the inset. Due to a protrusion in the center of the cell from the sealing process, magnets cannot be placed in this region. To ensure proper alignment, the magnets must be evenly spaced while preventing the cell from extending beyond the outer edge of the magnet array.

When the cell extends beyond the magnet array, stray magnetic field lines that do not pass through the central holes can interact with the atoms. These field lines are oriented opposite to the main field inside the rings, causing the direction of the peak shift to reverse.

A different effect arises when only two magnets are used. In this case, even if the cell is properly aligned, the magnetic field lines inside the two rings fail to connect smoothly. As a result, the space between the magnets is dominated by field lines oriented opposite to those within the rings, leading to a reversal of the DAVLL peak shift. This reversal is most evident in the $F''=3 \rightarrow F'=4$ transition, which shows particularly high

sensitivity to magnetic field variations. Increasing the number of magnets to four or more improves the continuity of the magnetic field inside the rings, suppressing the influence of these opposing field lines and stabilizing the DAVLL signal.

The apparent magnitude of the peak shift in response to the magnetic field varies depending on the hyperfine levels involved in the transition. Among the observed transitions, the $F''= 3 \rightarrow F'= 4$ line exhibited the largest peak shift, making it the most suitable for generating a DAVLL signal. This can be attributed to Zeeman-selective optical pumping between stretched-state sublevels, which behaves nearly closed on the experimental time scale. For the $F''= 3 \rightarrow F'= 4$ transition, σ^+ and σ^- components drive resonant transitions between $m_{F''}= +3 \rightarrow m_{F'} = +4$ and $m_{F''} = -3 \rightarrow m_{F'} = -4$, respectively. Because atoms excited to $m_{F'} = \pm 4$ predominantly decay back to $m_{F''} = \pm 3$, Zeeman-selective optical pumping between the stretched states is strongly enhanced compared with other hyperfine lines. Consequently, the DAVLL signal for the $F''= 3 \rightarrow F'= 4$ transition closely approximates the ideal dichroic response to a magnetic field. Furthermore, increasing the magnetic field strength widens the separation between Signal 1 and Signal 2, improving the signal slope available for frequency locking.

On the other hand, the $F''= 3 \rightarrow F'= 3$ and $F''= 4 \rightarrow F'= 4$ transitions do not support effective Zeeman-selective optical pumping, resulting in only minimal peak shifts under the magnetic field—so small that they are barely observable. Consequently, the slope of the DAVLL signal, which is essential for wavelength stabilization, cannot be effectively obtained from these lines.

In the $F''= 4 \rightarrow F'= 3$ transition, efficient Zeeman-selective optical pumping does not occur. However, σ^+ and σ^- components can still drive transitions between $m_{F''} = +4 \rightarrow m_{F'} = +3$ and $m_{F''} = -4 \rightarrow m_{F'} = -3$, respectively. As a result, although the response to the magnetic field is weaker than that of the $F'' = 3 \rightarrow F' = 4$ transition, a finite degree of peak shift is still observable. In our experiment, however, Signal 1 was strongly suppressed, preventing the formation of a clean DAVLL signal.

Among the results obtained in this experiment, the $F'' = 3 \rightarrow F' = 4$ transition with four magnets produced the most suitable error signal for wavelength stabilization. The gradient of its DAVLL signal coincides with the intrinsic absorption peak of cesium and, importantly, does not depend on the stability of any single Signal. If the DAVLL signal were dominated by one component, it would be highly sensitive to fluctuations in cesium vapor pressure, since temperature variations in the cell strongly affect peak heights. An ideal DAVLL signal, by contrast, should inherently cancel out such variations in amplitude, ensuring a stable error signal for feedback control.

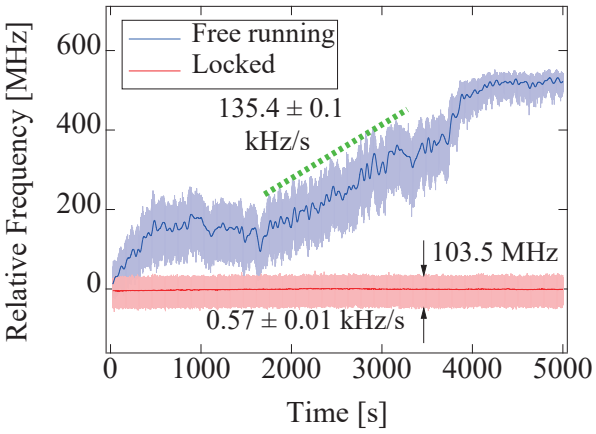

Fig. 6. Comparison of a VCSEL stabilized using the DAVLL signal with four magnets and an unstabilized VCSEL, evaluated from a reference signal aligned to the cesium absorption peak over 5000 s. The red trace shows the wavelength variation of the stabilized VCSEL, and the blue trace that of the free-running VCSEL (temperature-controlled only). The central red and blue curves indicate moving averages of the respective data. The green line represents the fitted slope of the evaluated section of the free-running case.

Figure 6 shows the evaluation of VCSEL wavelength shift with and without wavelength stabilization. The graph plots elapsed time on the horizontal axis and relative frequency, derived from the cesium absorption spectrum, on the vertical axis. The DAVLL signal was generated using four magnets, with the servo controller time constant set to 100 Hz.

When wavelength locking was applied, the VCSEL exhibited a linewidth of 103.5 MHz and a drift rate of 0.57 kHz/s. For comparison, in the free-running state the drift rate reached a maximum of 135.4 kHz/s. As seen by comparing with the inset of

Figure 4, the laser spectrum linewidth remained nearly unchanged, but the drift was significantly suppressed. The slightly narrower linewidth observed in the locked case is likely an artifact: because the VCSEL frequency is stabilized near the cesium absorption peak, noise-induced fluctuations appear smaller than those in the side-fringe region.

4 Discussion

The experimental results demonstrate that a low-cost and simple wavelength standard for the cesium D_1 line can be realized using a VCSEL and DAVLL. This approach is particularly valuable in experiments where continuous wavelength scanning is not feasible, but frequency tuning within the GHz range is needed to track long-term responses. One such case is Light-Induced Drift (LID), for which this wavelength standard was specifically developed to enable real-time determination of laser frequency using a Fabry–Perot interferometer in combination with a stabilized reference laser. Although VCSELs exhibit significant current noise that makes linewidth narrowing difficult, this is not a critical limitation for standardization purposes. The observed drift rate demonstrates that the system provides sufficient stability for practical applications.

Single-mode VCSELs are now available at relatively low cost for selected wavelengths, including the Cs D_1, Cs D_2, and Rb D_1 lines. While variations in output wavelength exist between individual devices, the available tuning range of ~3.5 nm within the temperature-tuning range provided by the Peltier element demonstrates that such tuning is feasible for typical VCSEL samples under proper temperature control. The main limitation of VCSELs is their susceptibility to current noise, which makes them unsuitable for techniques requiring extreme spectral resolution, such as sub-Doppler DAVLL. In this study, permanent magnets were chosen to generate the magnetic field, avoiding the heating issues of current-driven coils. Proper arrangement of the magnets was crucial to ensure smooth magnetic field line continuity, and four evenly spaced magnets around a 10 cm cell were found to yield the most stable DAVLL signal. Adding more magnets increased the apparent shift but introduced peak broadening, making the four-magnet configuration optimal.

The response of spectral peaks to the magnetic field is strongly influenced by the hyperfine quantum numbers. The $F'' = 3 \rightarrow F' = 4$ transition, which exhibits Zeeman-selective optical pumping between stretched sublevels that behaves nearly closed on the experimental time scale, produced the most ideal DAVLL signal. In contrast, the $F'' = 3 \rightarrow F' = 3$ and $F'' = 4 \rightarrow F' = 4$ transitions exhibited negligible shifts, while the $F'' = 4 \rightarrow F' = 3$ transition showed partial polarization dependence but yielded a distorted signal unsuitable for stabilization. For the cesium D_2 line, both lower-state transitions have closed cycling transitions, making ideal DAVLL signals easier to obtain [18]. By contrast, in the D_1 line, only specific transitions support efficient Zeeman-selective optical pumping, limiting the conditions under which an ideal signal emerges. At the same time, the well-separated hyperfine transitions in the D_1 line allow a clearer observation of the link between quantum numbers and dichroic response. In systems without cycling transitions, Zeeman-selective optical pumping plays an essential role in the formation of DAVLL signals.

5 Conclusions

In this study, we demonstrated a low-cost and straightforward wavelength standard for the cesium D_1 line using a single-mode VCSEL in combination with DAVLL. By optimizing the magnetic field with a ring-shaped permanent magnet array, a stable DAVLL signal was obtained from the $F'' = 3 \rightarrow F' = 4$ transition, where Zeeman-selective optical pumping between stretched sublevels behaves nearly closed on the experimental time scale, enhancing the dichroic response. The system achieved wavelength stabilization with a drift rate of ~0.57 kHz/s. Although the VCSEL exhibited a relatively broad linewidth due to current noise, this did not hinder its performance as a wavelength reference. The results confirm that such a compact system can provide sufficient long-term stability for practical

applications, particularly as a reference subsystem in experiments such as Light-Induced Drift (LID), where continuous wavelength scanning is not feasible. This approach may also serve as a model for applying inexpensive VCSEL-based standards in other spectroscopic experiments requiring robust but low-cost frequency stabilization.

Acknowledgements

We would like to express our gratitude to Shogo Horikane for his support during the early stages of this experiment. This work was supported by JSPS KAKENHI Grant Number JP21K04947.

References

[1] A. H. Rawicz, *Proc. of SPIE*. 713802-1 (2008).
[2] S. Chu, L. Hollberg, J. E. Bjorkholm, A. Cable, and A. Ashkin, *Phys. Rev. Lett.*, **55**, 48–51 (1985).
[3] E. A. Cornell and C. E. Wieman, *Rev. Mod. Phys.*, **74**, 875–893 (2002).
[4] J. L. Hall, L. Hollberg, T. Baer, and H. G. Robinson, *Appl. Phys. Lett.*, **39**, 680–682 (1981).
[5] H.-R. Noh, S. E. Park, L. Z. Li, J. D. Park, and C. H. Cho, *Opt. Express*, **19**, 23444–23452 (2011).
[6] V. Negnevitsky and L. D. Turner, *Opt. Express*, **21**, 3103–3113 (2013).
[7] B. Chéron, H. Gilles, J. Hamel, O. Moreau, and H. Sorel, *J. Phys. III France*, **4**, 401–406 (1994).
[8] K. L. Corwin, Z. T. Lu, C. F. Hand, R. J. Epstein, and C. E. Wieman, *Appl. Opt.*, **37**, 3295–3298 (1998) .
[9] J. M. Reeves, O. Garcia, and C. A. Sackett, *Appl. Opt.*, **45**, 372–376 (2006).
[10] S. Yin, H. Liu, J. Qian, T. Hong, Z. Xu, and Y. Wang, *Opt. Commun.*, **285**, 5169–5174 (2012).
[11] S. Pustelny, V. Schultze, T. Scholtes, and D. Budker, *Rev. Sci. Instrum.*, **87**, 063107 (2016).
[12] T. Hasegawa and M. Deguchi, *J. Opt. Soc. Am. B*, **26**, 1216–1220 (2009).
[13] S. Okubo, K. Iwakuni, and T. Hasegawa, *Opt. Commun.*, **285**, 4107–4111 (2012).
[14] C. Lee, G. Z. Iwata, E. Corsini, J. M. Higbie, S. Knappe, M. P. Ledbetter, and D. Budker, *Rev. Sci. Instrum.*, **82**, 043107 (2011).
[15] D.-Q. Su, T.-F. Meng, Z.-H. Ji, J.-P. Yuan, Y.-T. Zhao, L.-T. Xiao, and S.-T. Jia, *Appl. Opt.*, **53**, 7011–7016 (2014).
[16] K. Iga, *Jpn. J. Appl. Phys.*, **47**, 1–10 (2008).
[17] K. Yuki, T. Kobayashi, and L. Matsuoka, *J. Nucl. Sci. Technol.*, **54**, 1240–1250 (2017).
[18] Y. Kusano, N. Nishiya, and L. Matsuoka, *IOP Conf. Ser.: Mater. Sci. Eng.*, **625**, 012007 (2019).